Fig. S1

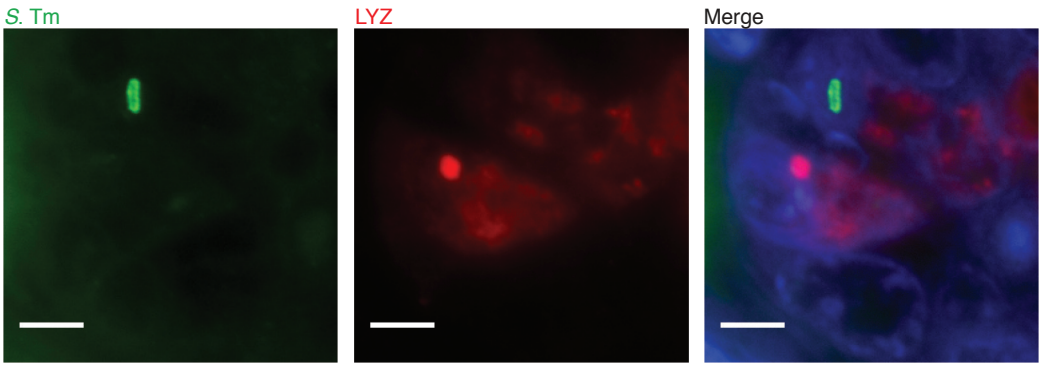

Figure S1: *S.* Typhimurium invades Paneth cells. Immunofluorescence detection of *S.* Typhimurium and lysozyme (LYZ) in infected mouse small intestinal crypts. Nuclei are stained with DAPI. Scale bars=5 µm. *S.* Tm, *Salmonella* Typhimurium.

Fig. S2

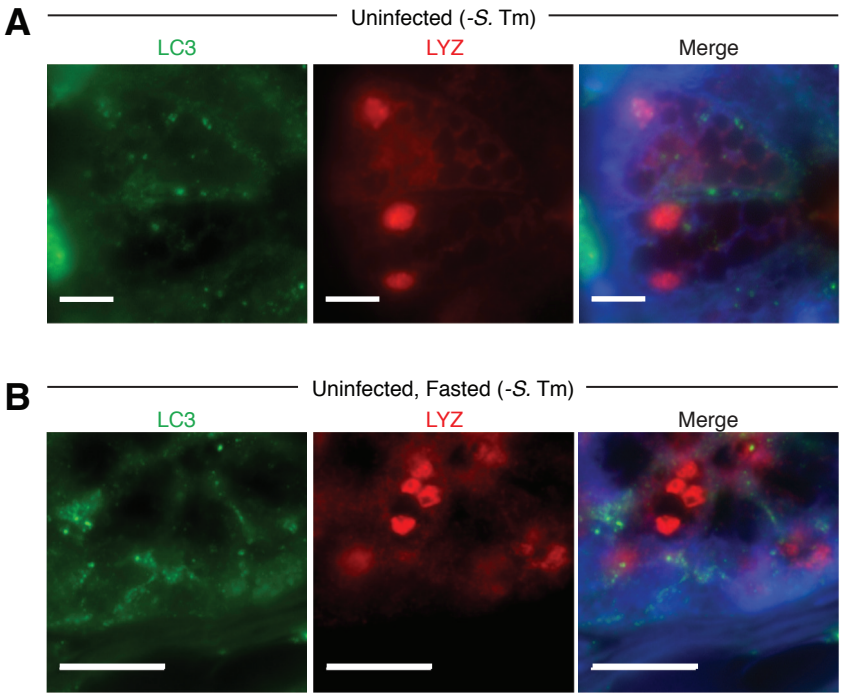

Figure S2: Lysozyme is packaged into LC3$^-$ secretory granules in uninfected mice. Immunofluorescence detection of LC3 and lysozyme in small intestinal crypts of uninfected **(A)** and fasted **(B)** mice. Nuclei are stained with DAPI. Scale bars=10 μm. *S.* Tm, *Salmonella* Typhimurium; LYZ, lysozyme.

Fig. S3

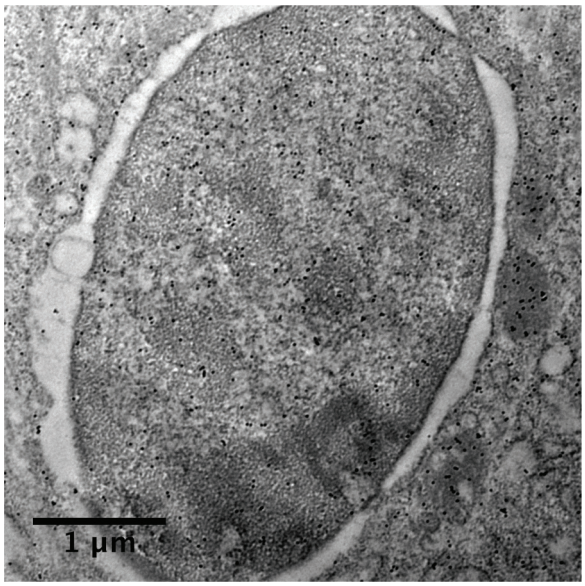

Figure S3: Unconventional secretory granules in Paneth cells of *S.* Typhimurium-infected mice contain lysozyme. Transmission electron microscopy of immunogold-labeled lysozyme in a Paneth cell from a *S.* Typhimurium-infected mouse.

Fig. S4

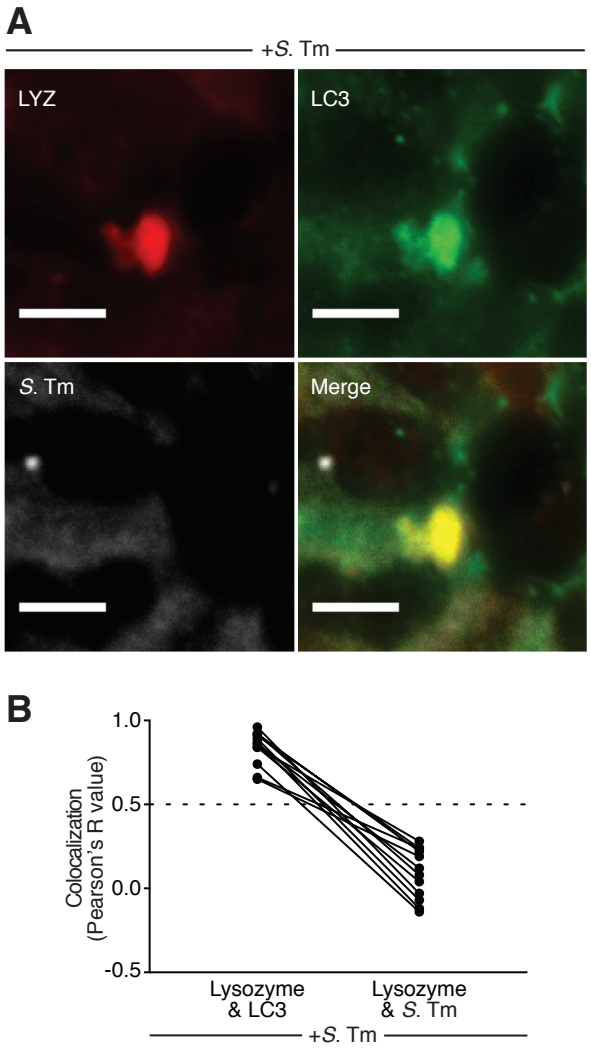

Figure S4: *S.* Typhimurium does not colocalize with lysozyme-filled LC3$^+$ vesicles in Paneth cells. (A) Immunofluorescence detection of *S.* Typhimurium, LC3 and lysozyme in infected mouse small intestinal crypts. Scale bars=5 μm. **(B)** Quantification of *S.* Typhimurium, LC3 and lysozyme colocalization in **A**. Each point represents one lysozyme-containing granule. Two points connected by a line represent the same granule. Two events were analyzed per mouse. Dotted line represents limit of strong colocalization. *S.* Tm, *Salmonella* Typhimurium; LYZ, lysozyme.

Fig. S5

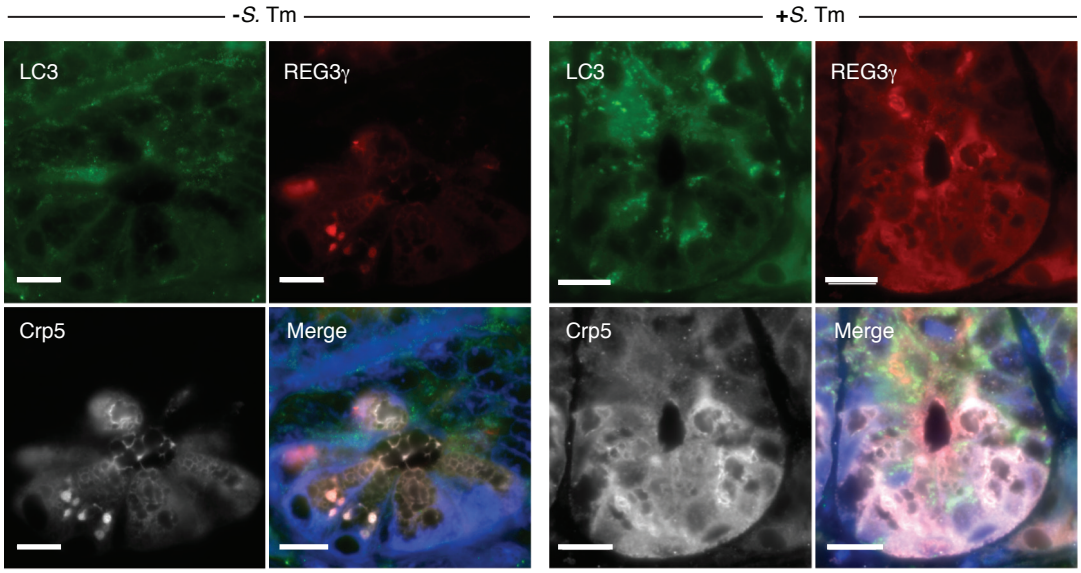

Figure S5: REG3γ and Crp5 are packaged in LC3$^-$ secretory granules in Paneth cells from uninfected mice but are diffused throughout the cytoplasm in *S.* Typhimurium-infected mice. Immunofluorescence detection of LC3, cryptdin 5 (Crp5) and REG3γ in small intestinal crypts. Nuclei are stained with DAPI. Scale bars=10 μm. *S.* Tm, *Salmonella* Typhimurium; Crp5, cryptdin 5.

Fig. S6

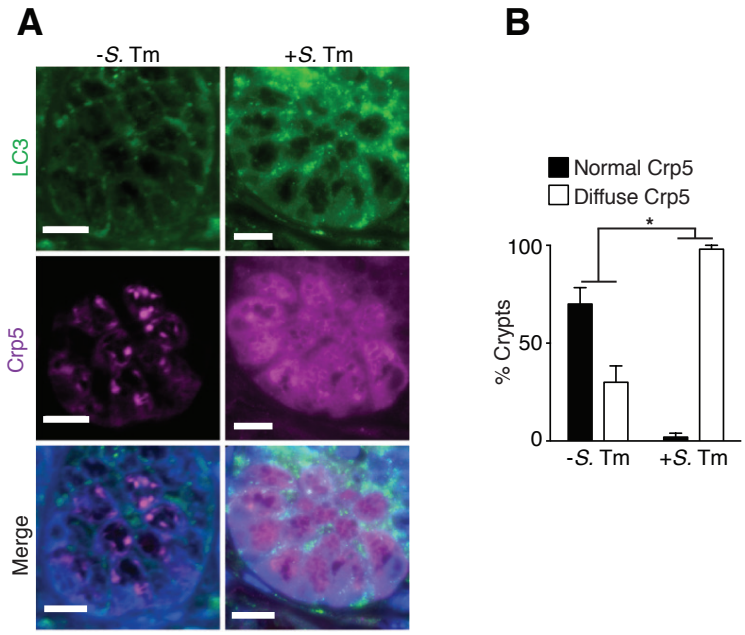

Figure S6: Cryptdin-5 is excluded from secretory granules in Paneth cells from *S.* Typhimurium infected mice. (A) Immunofluorescence detection of LC3 and cryptdin-5 (Crp5) in mouse small intestinal crypts. Scale bars=10 μm. **(B)** Quantification of small intestinal crypts displaying a diffuse cryptdin-5 signal. *$p<0.05$; Two-way ANOVA.

Fig. S7

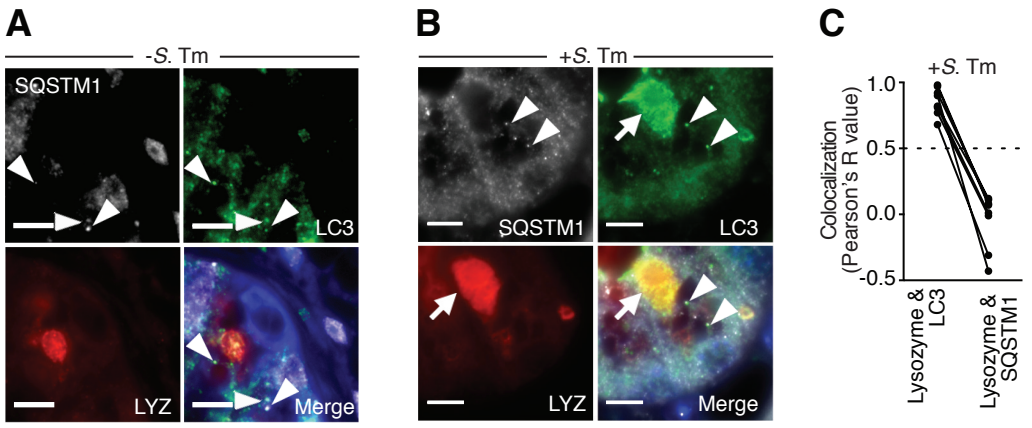

Figure S7: SQSTM1 (p62) does not colocalize with lysozyme-filled LC3$^+$ vesicles in Paneth cells from *S.* Typhimurium infected mice. (A) Immunofluorescence detection of SQSTM1, LC3 and lysozyme in uninfected mouse small intestinal crypts, showing that SQSTM1 colocalizes with LC3 but not lysozyme in Paneth cells from uninfected mice. Nuclei are stained with DAPI. Arrowheads indicate LC3$^+$ vesicles colocalizing with SQSTM1 but not lysozyme. **(B)** Immunofluorescence detection of SQSTM1, LC3 and lysozyme in *S.* Typhimurium-infected mouse small intestinal crypts. Arrows indicate a lysozyme-filled LC3$^+$ vesicle with no SQSTM1 signal. Arrowheads indicate LC3$^+$ vesicles colocalizing with SQSTM1 but not lysozyme. **(C)** Quantification of SQSTM1, LC3 and lysozyme colocalization in **B**. Each point represents one lysozyme-containing granule. Two points connected by a line represent the same granule. Two events were analyzed per mouse. Dotted line represents limit of strong co-localization. Scale bars=5 μm. *S.* Tm, *Salmonella* Typhimurium; LYZ, lysozyme.

Fig. S8

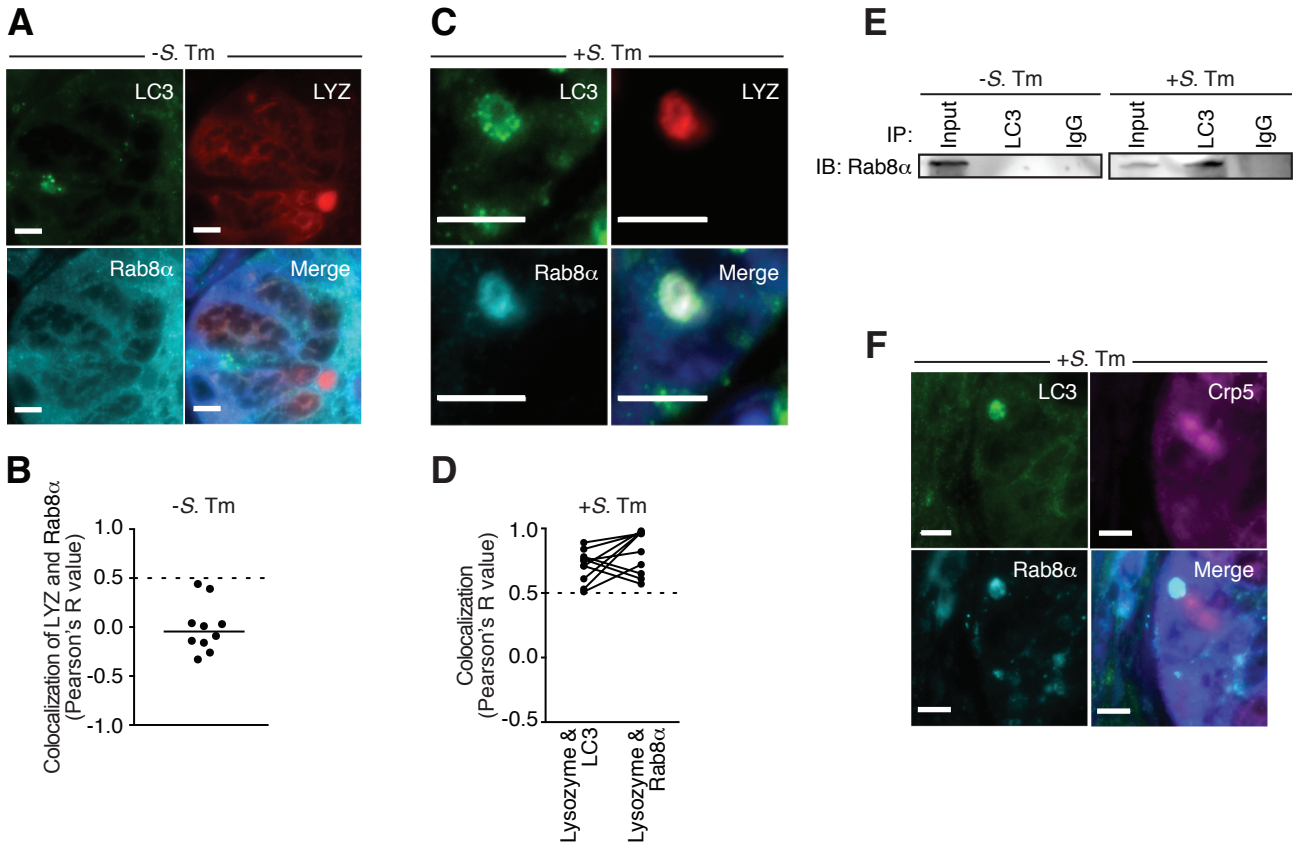

Figure S8: Rab8α colocalizes with lysozyme-filled LC3⁺ vesicles, but not cryptdin-5 in Paneth cells from *S.* Typhimurium infected mice. (A) Immunofluorescence detection of Rab8α, LC3 and lysozyme in uninfected mouse small intestinal crypts. Nuclei are stained with DAPI. Scale bars=5 μm. **(B)** Quantification of Rab8α and lysozyme colocalization in **A**. Each point represents one lysozyme-containing granule. Two events were analyzed per mouse. Dotted line represents limit of strong colocalization. **(C)** Immunofluorescence detection of Rab8α, LC3 and lysozyme in *S.* typhimurium-infected mouse small intestinal crypts. Scale bars=5 μm. **(D)** Quantification of Rab8α, LC3 and lysozyme co-localization in **C**. Each point represents one lysozyme-containing granule. Two points connected by a line represent the same granule. Two events were analyzed per mouse. Dotted line represents limit of strong co-localization. **(E)** Co-immunoprecipitation of small intestinal lysates using the indicated antibodies. Immunoblot was detected using anti-Rab8α antibody. Blot is representative of 3 independent experiments. **(F)** Immunofluorescence detection of Rab8α, LC3 and cryptdin 5 (Crp5) in *S.* Typhimurium-infected mouse small intestinal crypts. Nuclei are stained with DAPI. Scale bars=5 μm. *S.* Tm, *Salmonella* Typhimurium; LYZ, lysozyme; Crp5, cryptdin-5.

Fig. S9

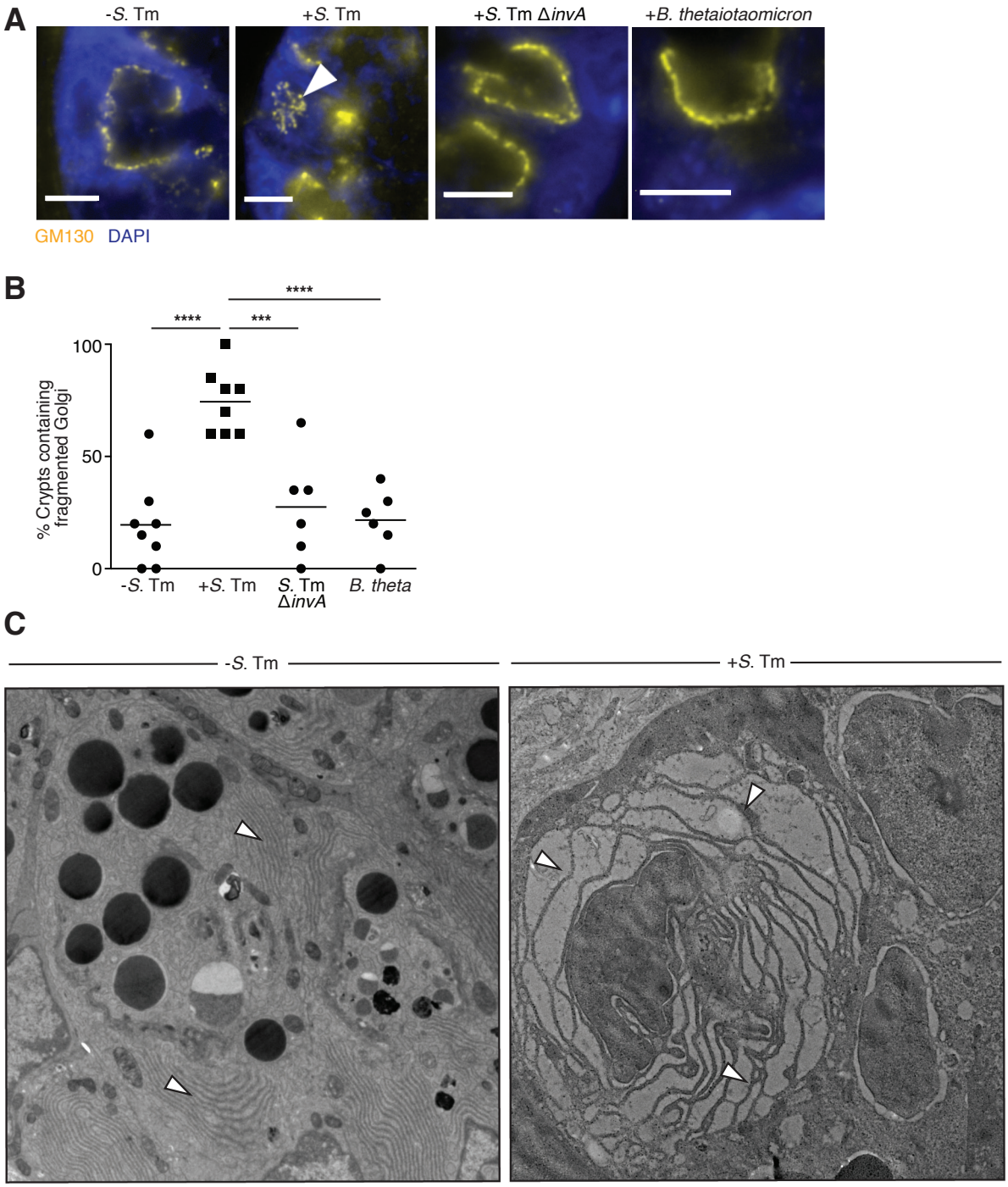

Figure S9: *Salmonella* Typhimurium infection causes Golgi fragmentation in Paneth cells. **(A)** Immunofluorescence detection of the Golgi marker GM130 in Paneth cells of infected and uninfected mice. Nuclei are stained with DAPI. Scale bars=5 μm. Arrowhead indicates fragmented Golgi. **(B)** Quantification of small intestinal crypts displaying fragmented Golgi. Each dot represents one mouse. 20 Crypts were analyzed per mouse. **(C)** Transmission electron microscopy of Paneth cells in small intestinal crypts of uninfected and infected mice. Arrowheads indicate Golgi cisternae. ***p<0.001, ****p<0.0001; One-way ANOVA. *S.* Tm, *Salmonella* Typhimurium; *B. theta*, *Bacteroides thetaiotaomicron*.

Fig. S10

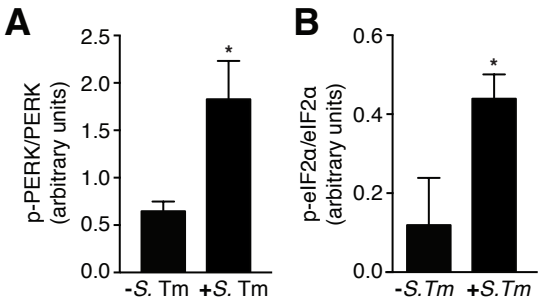

Figure S10: Infection of mice with *S.* Typhimurium induces PERK and eIF2α phosphorylation. Quantification of immunoblot detection of PERK and p-PERK **(A)** and eIF2α and p-eIF2α **(B)**. Three independent experiments were run, and a representative immunoblot is shown in **Fig. 3F**. Error bars represent SEM. *p<0.05; Student's t-test. *S.* Tm, *Salmonella* Typhimurium.

Fig. S11

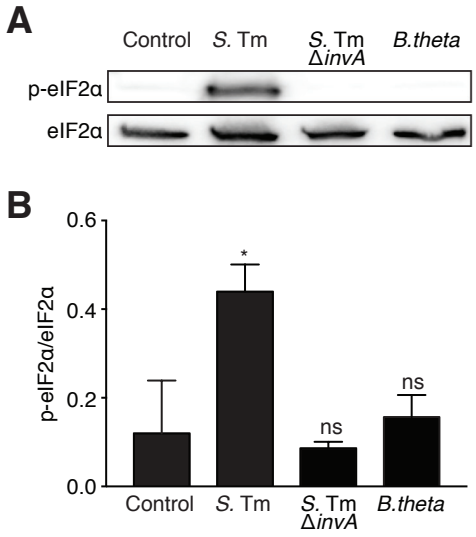

Figure S11: Infection of mice with non-invasive bacteria (*S.* Typhimurium Δ*invA* or *Bacteroides thetaiotaomicron)* does not induce eIF2α phosphorylation. (A) Representative immunoblot of small intestines from mice orally challenged with the indicated bacteria. **(B)** Quantification of immunoblots represented in **A**. Error bars represent SEM. *p<0.05; One-way ANOVA. *S.* Tm, *Salmonella* Typhimurium; *B. theta*, *Bacteroides thetaiotaomicron.*

Fig. S12

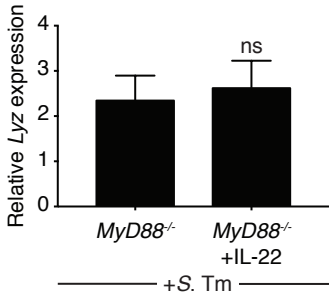

Figure S12: IL-22 treatment does not alter *lysozyme* transcript abundance in infected *MyD88*$^{-/-}$ mice. Relative *lysozyme* transcript levels in *S.* Typhimurium-infected *MyD88*$^{-/-}$ mice treated as indicated. Error bars represent SEM. ns, not significant; Student's t-test. *S.* Tm, *Salmonella* Typhimurium.

Fig. S13

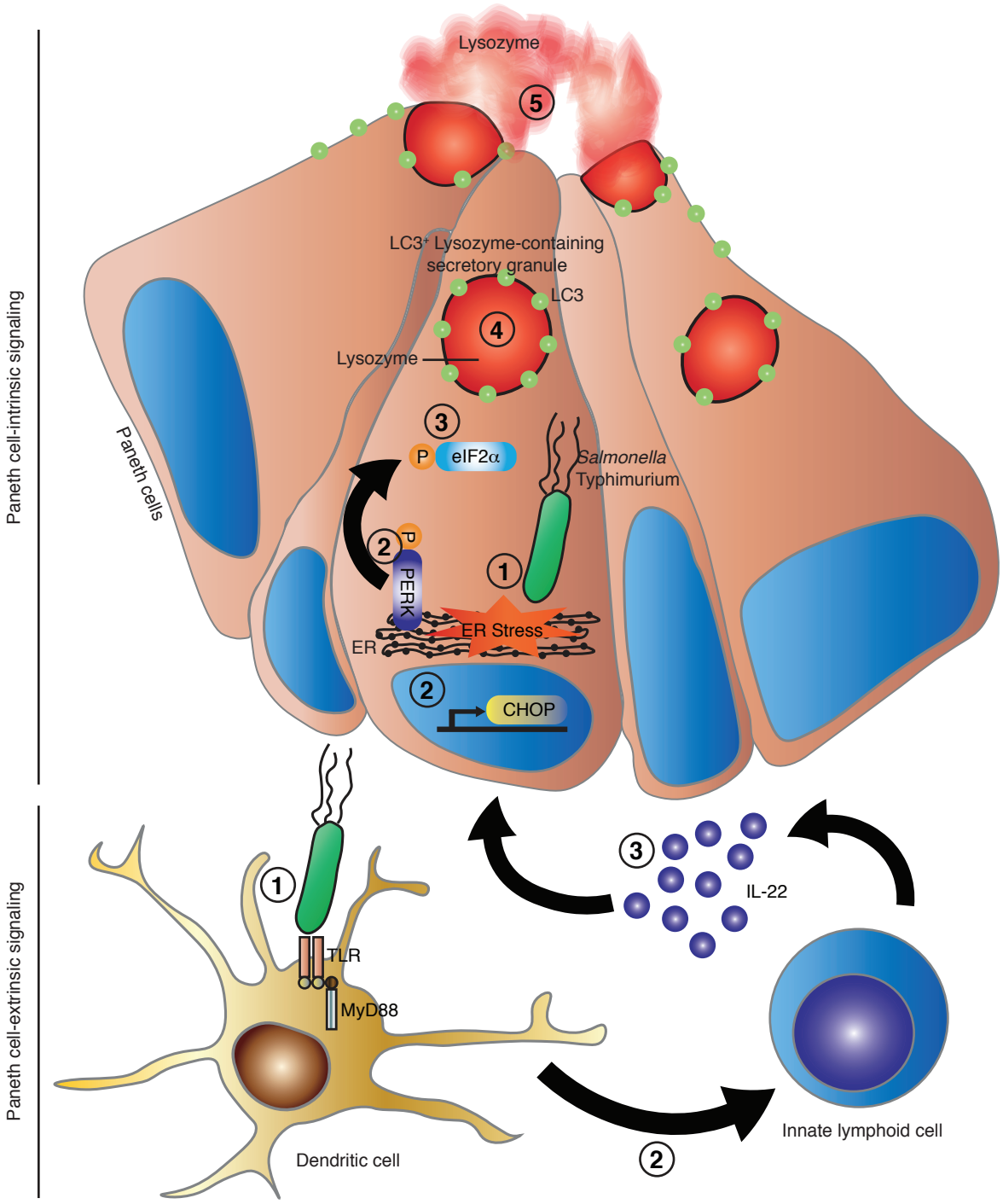

Figure S13: Model of the pathways that regulate secretory autophagy of lysozyme in Paneth cells. ***Paneth cell-intrinsic signaling:*** **(1)** Invasion by a pathogen such as *Salmonella* Typhimurium damages the Golgi apparatus and causes endoplasmic reticulum (ER) stress. **(2)** ER stress leads to upregulation of CHOP expression, PERK phosphyorylation and **(3)** eIF2α phosphorylation, which is required for **(4)** packaging of lysozyme in $LC3^+$ vesicles that **(5)** deliver lysozyme to the apical cell surface. ***Paneth cell-extrinsic signaling:*** **(1)** Bacterial signals are captured by dendritic cell TLRs and **(2)** relayed to innate lymphoid cells that produce IL-22. **(3)** IL-22 licenses Paneth cells to activate secretory autophagy upon detection of ER stress.

Fig. S14

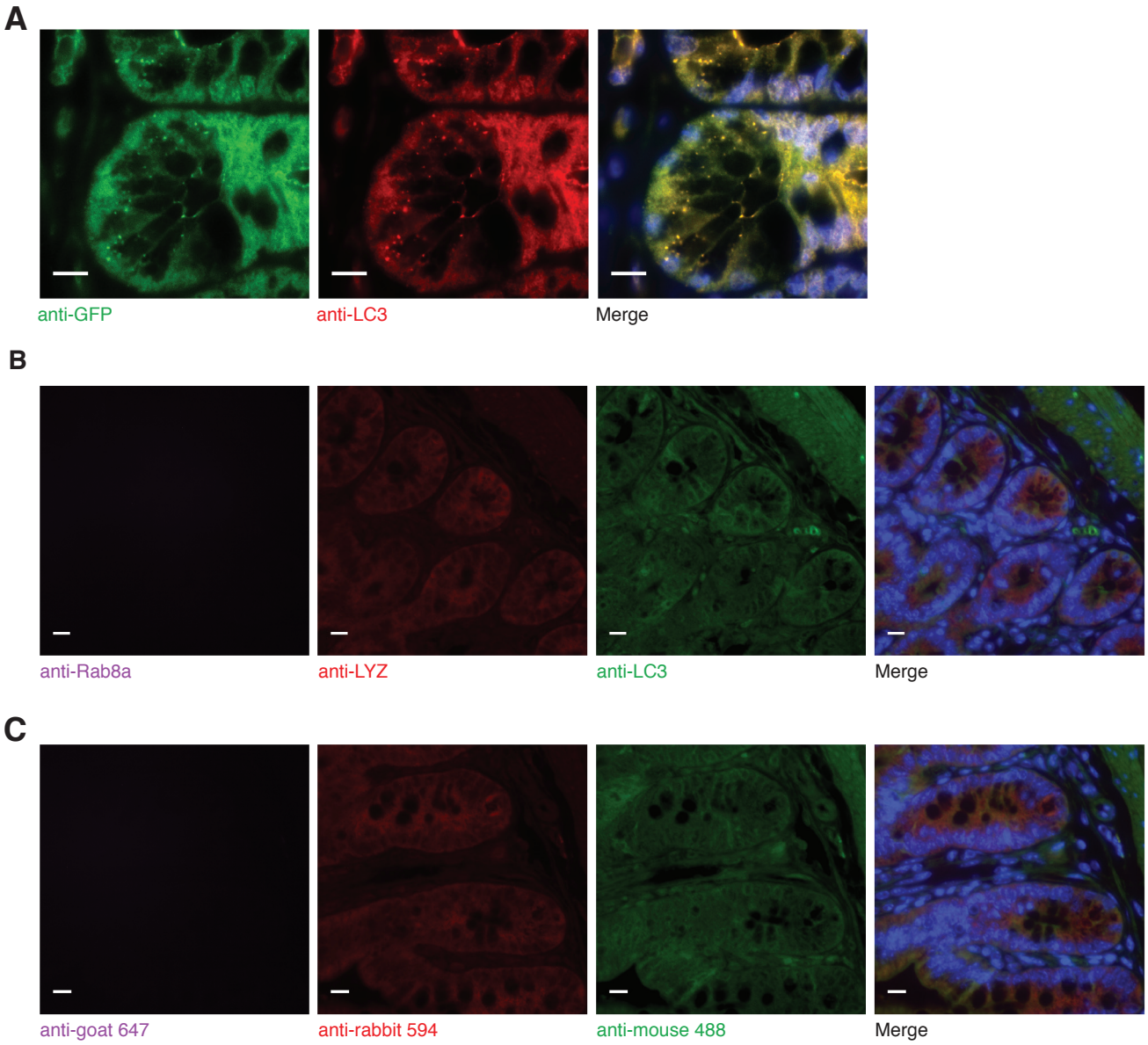

Figure S14: Antibody validation. (A) Immunofluorescence detection of GFP (green) and LC3 (red) in small intestinal tissue of a LC3-GFP mouse. Nuclei are stained with DAPI. Scale bars=10 μm **(B)** Immunofluorescence detection of the indicated primary antibodies using no secondary antibody in mouse small intestinal tissue. Nuclei are stained with DAPI. Scale bars=10 μm **(C)** Immunofluorescence detection of the indicated secondary antibodies using no primary antibody in mouse small intestinal tissue. Nuclei are stained with DAPI. Scale bars=10 μm.